DOI 10.1007/s11595-014-0861-3

Electrochemical Preparation and Photoelectric Properties of Cu_2O-loaded TiO_2 Nanotube Arrays

LI Guangliang, LIANG Wei*, XUE Jinbo, LIU Yiming, LIANG Xingzhong
(College of Materials Science and Engineering, Taiyuan University of Technology, Taiyuan 030024, China)

Abstract: TiO_2 nanotube (TNT) arrays were fabricated by anodic oxidation of titanium foil in a fluoride-based solution, on which Cu_2O particles were loaded via galvanostatic pulse electrodeposition in cupric acetate solutions in the absence of any other additives. The structure and optical properties of Cu_2O-loaded TiO_2 nanotube arrays (Cu_2O-TNTs) were analyzed by scanning electron microscopy (SEM), X-ray diffraction (XRD) and UV-Vis absorption, and the photoelectrochemical performance was measured using an electrochemical work station with a three-electrode configuration. The results show that the Cu_2O particles distribute uniformly on the highly ordered anatase TiO_2 nanotube arrays. The morphologies of Cu_2O crystals change from branched, truncated octahedrons to dispersive single octahedrons with increasing deposition current densities. The Cu_2O-TNTs exhibited remarkable visible light responses with obvious visible light absorption and greatly enhanced visible light photoelectrochemical performance. The I-V characteristics under visible light irradiation show a distinct plateau in the region between approximately −0.3 and 0 V, resulting in higher open-circuit voltages and larger short-circuit currents with increased Cu_2O deposition.

Key words: TiO_2 nanotube arrays; Cu_2O crystals; anode oxidation; electrodeposition; photocurrent

1 Introduction

Since the discovery of carbon nanotube in 1991[1], nanotubular structures have been researched extensively due to their excellent physical and chemical properties for potential applications in sensors, catalysis and photoelectric conversion. Among the various nanotubular materials, TiO_2 nanotube (TNT) arrays have attracted intensive and continuous attention in the areas of photocatalysis[2-4], direct ethanol fuel cell (DEFC)[5] and solar energy conversion[6, 7] in recent decades because of their advantages over traditional TiO_2 films. Different geometrical shapes of titania nanotubes have been prepared by various methods, including hydrothermal synthesis[8,9], sol-gel processing[10,11] and anodic oxidation[12-14]. Among these synthetic techniques, anodic oxidation has been the most commonly used preparation method for substrate-supported TiO_2 nanotube arrays. However, as a wide-bandgap semiconductor (3.2 eV for anatase), TiO_2 absorbs only the ultraviolet light which accounts for only 3%-4% of the total incident sunlight, resulting in a very low photocatalytic efficiency outdoors. In addition, its high recombination rate of photoinduced electron-hole pairs greatly reduces its energy conversion efficiency. Therefore, attempts have been made to improve the charge separation efficiency and the visible light absorption of TiO_2[5, 6]. To form a heterojunction structure between TNT and other narrow bandgap semiconductors with matched band potentials may provide an effective way to solve these problems.

Cuprous oxide (Cu_2O) is a well-known non-toxic and low cost p-type semiconductor with a direct band gap of 2.1 eV, and has emerged as a promising material for using visible light to produce photoelectrons

(Received: Jan. 19, 2013; Accepted: Oct. 8, 2013)
LI Guangliang (李光亮): E-mail: liguangliang126@126.com.
*Corresponding author: LIANG Wei (梁伟): Prof.; Ph D; E-mail: liangwei@tyut.edu.cn
Funded by the National Natural Science Foundation of China (No. 51175363), the Youth Staff Fund of Taiyuan University of Technology (Nos. K201016, K201013), the Specialized Fund for Innovative of College Students of Taiyuan City (No. 09122018), the Program for Changjiang Scholar and Innovative Research Team in University (No. IRT0972)

generation[15, 16]. Furthermore, both the conduction band potential and the valence band potential of TiO_2 are more positive than the corresponding bands of Cu_2O, which allows for efficient electron transfer between the two semiconductors. T Mahalingam *et al* synthesized Cu_2O film on Cu and tin oxide coated substrates by electrochemical pulse plating techniques[17]. Recently, Hou *et al*[18] loaded Cu_2O nanoparticles on TNT arrays surfaces by photocatalytic reduction with $CuSO_4$, methanol and a phosphate buffer solution, and the heterojunction arrays exhibited effective photocatalytic and promoted photoelectric properties under the visible light.

As we have known, almost all of the above reports focus on either the assistance of buffer solutions or the requirement of alkaline solution, or even application of elevated temperatures when necessary. During deposition, Cu^{2+} ions are first reduced to Cu^+ ions (Eq.1), and Cu^+ ions are then precipitated from solution to form Cu_2O (Eq.2). From (Eq.2), we can see that H^+ ions are produced with the formation of Cu_2O, which results in a local pH decrease around the working electrode. This hinders the formation of Cu_2O, and thus, buffered plating media or alkaline solutions are introduced to maintain the pH around the working electrode (Eqs.3-4).

$$Cu^{2+}+e^- \longleftrightarrow Cu^+ \quad (1)$$

$$2Cu^++H_2O \longleftrightarrow Cu_2O+2H^+ \quad (2)$$

$$CH_3COO^-+H^+ \longleftrightarrow CH_3COOH \quad (3)$$

$$OH^-+H^+ \longleftrightarrow H_2O \quad (4)$$

In this paper, we report a facile route for the preparation of Cu_2O/ TiO_2 nanotube arrays by anodic oxidation of titanium in NH_4F and H_3PO_4 aqueous solutions followed by a subsequent electrodeposition with a cupric acetate aqueous solution without any extra additives. The cupric acetate aqueous solution plays a dual role in the deposition of Cu_2O, serving as both the working electrolyte and a buffer solution. This means that the acetate ions work as H^+ ion scavengers so that the local pH value around the working electrode remains constant during the deposition. This occurs because the H^+ ions produced in Eq.(2) are consumed in Eq.(3). This provides a suitable condition for the deposition of octahedral Cu_2O.

2 Experimental

2.1 Preparation of TiO_2 nanotube arrays

The TiO_2 nanotube arrays were fabricated by electrochemical anodization of 99% pure titanium plates. The titanium plates, 13 mm×30 mm×0.3 mm, were ground, finely polished, and rinsed in an ultrasonic bath in acetone for 20 min, ethanol for 10 min and finally deionized water for 5 min, respectively.

The anodization was performed in a two-electrode electrochemical cell with a platinum cathode. The clean titanium plates were first anodized at a constant 20 V potential in a 0.25 M H_3PO_4 (100 mL) electrolyte solution at 40 ℃ for 5 min. Then, 0.02 mol NH_4F was added to the electrolyte, and anodization was continued for 4 h. During these processes, the electrolytes were constantly stirred at a rate of 40 rpm. The distance between the two electrodes was 3 cm. After anodization, the samples were rinsed with deionized water and dried in air. To obtain a crystalline nanotubular structure, all samples were annealed at 500 ℃ for 2 h in air in a resistance furnace (SX-2-5-12). The heating and cooling rates were maintained at 2 ℃/ min. In this paper, the annealed samples are denoted to as A-TNT.

2.2 Deposition of Cu_2O

Cu_2O was deposited onto the annealed TiO_2 nanotubes arrays (A-TNT) via the galvanostatic pulse electrodeposition method using a $Cu(CH_3COO)_2$ solution as the working electrolyte at ambient temperature. The working electrolyte was prepared as follows: 0.399 3 g $Cu(CH_3COO)_2 \cdot H_2O$ (A.P.) was added to 100 mL deionized water, and this solution was magnetically stirred at a rate of 100 rpm for 10 min. After agitation, the electrolyte was allowed to stand for 30 min before filtered. Electrodeposition was performed in a conventional three-electrode cell, with A-TNT as the working electrode, platinum foil as the counter electrode and a saturated calomel electrode (SCE) as the reference electrode. The deposition current density range from 0.2 to 1.5 mA/cm^2, and the deposition time for each sample was 5 min. The pulsed anode and cathode deposition time were set to 0.1 and 0.9 s, respectively. After deposition, the samples were soaked in ethanol for 5 min and then dried in air. The deposited samples are designated as D-TNT.

2.3 Microstructure characterization and photoelectric property measurement

Scanning electron microscopy images were obtained using a JEOL JSM-6700F field emitting scanning electron microscope (FESEM) operated at 10 kV. X-ray diffraction (XRD) patterns were recorded by a Bruker D8 diffractometer, (Cu Kα radiation). UV-Vis

absorption spectra were obtained using a Perkin Elmer Lambda 750 s spectrometer under diffuse reflectance mode. The photocurrent activity was measured on an electrochemical work station (CHI660D), using a neutral Na_2SO_4 aqueous solution (0.5 M) as the electrolyte, a platinum foil as the counter electrode, a saturated calomel electrode (SCE) as the reference electrode and a D-TNT as the working electrode. A 500 W Xe lamp (CHF-XW-500W) was used as the visible light source with the UV light being cutoff by a 400 nm optical filter.

3 Results and discussion

Fig.1 shows the current density-time curves for the H_3PO_4 electrolyte (a) and the mixed electrolyte (H_3PO_4 and NH_4F) (b) during the anodization of the titanium plate. Fig.1(a) shows that the current density increases steadily in the initial stage, and then slowly reaches a plateau at approximately 4 min, indicating the end of electrolytic polishing process. At the initial stage of anodization in the mixed electrolyte solution of H_3PO_4 and NH_4F (Fig.1(b)), the current density rapidly increases as the applied anodic potential increases from 0 to 20 V. The current density reaches its maximum value at about 0.5 min, followed by a drastic decrease to a minimum value within a few seconds, which may be attributed to the formation of a barrier layer on the surface of titanium. And then the current density slowly increases and reaches a plateau after approximately 2 min, possibly due to the reduction of the barrier layer thickness. This is followed by a gradual drop in the current density until the end of anodization. A similar phenomenon was also observed by Mor *et al*[19].

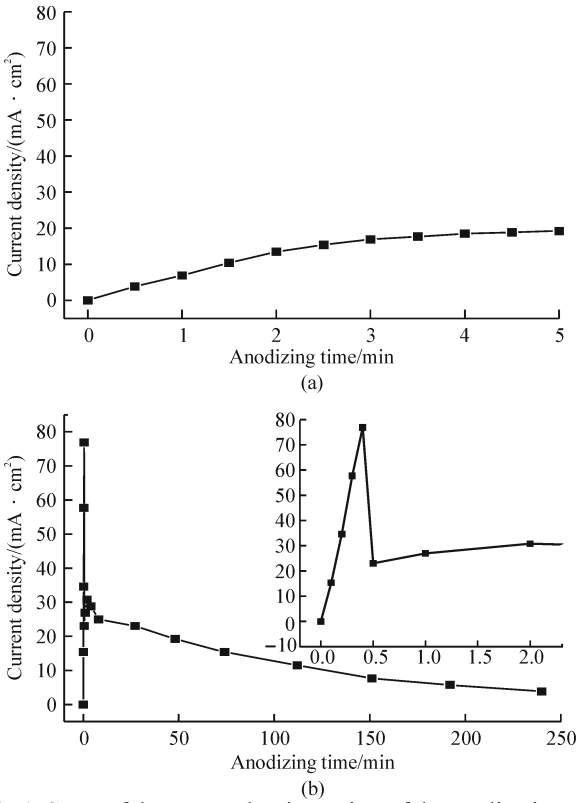

Fig.1 Curve of the current density *vs* time of the anodization of (a) H_3PO_4 electrolyte solution and (b) H_3PO_4 and NH_4F electrolyte solution (the inset is a magnified curve of the first few minutes of anodization)

SEM observation shows that the average diameter and length of tubes of A-TNTs are approximately 100 and 400 nm, respectively, as shown in Fig.2(a) and (b). For Cu_2O deposited samples (D-TNT), SEM observations show that a large number of Cu_2O nanoparticles are loaded on the surface of the tubular structures while some of them are inserted into the nanotubes, as shown in Fig.2(c)-(f).

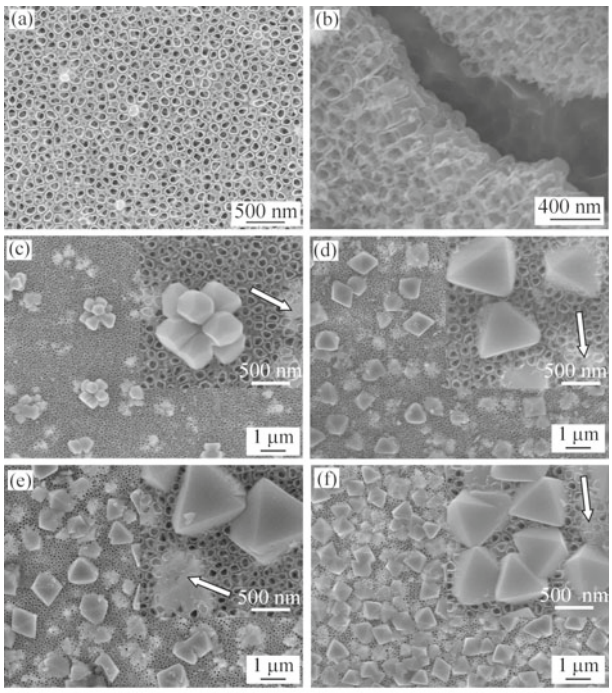

Fig.2 SEM images of A-TNT arrays ((a) and (b)), and D-TNT heterostructure arrays ((c) to (f)) fabricated with different current densities: (c) J=0.2 mA/cm^2, (d) J=0.5 mA/cm^2, (e) J=1.0 mA/cm^2 and (f) J=1.5 mA/cm^2. The inserts in (c)-(f) are representative SEM images

With a deposition current density of 0.2 mA/cm^2, the Cu_2O forms into branched, truncated octahedral shapes. As the current density increases, these particles gradually develop into dispersive single octahedron Cu_2O particles and the amount of Cu_2O particles increases apparently. When the current density values reach 1.5 mA/cm^2, large amounts of octahedral Cu_2O particles form and uniformly distribute on the surface of the TiO_2 naontube arrays. From Fig.2(c) - 2(f), it can be

seen that amorphous Cu_2O nanoparticles are assembled on the surface of TNT arrays prior to the formation of octahedral Cu_2O particles, as indicated by the arrows, implying that amorphous Cu_2O nanoparticles filled the TiO_2 naontubes and tubular interspaces. Compared with the work of Huang and co-workers[20], we were able to use a simpler synthetic route to obtain octahedral Cu_2O-modified TiO_2 NT arrays by galvanostatic pulse electrodeposition using a single electrolyte (slightly acidic cupric acetate aqueous solution) at ambient temperature.

The Cu^{2+} ions in the electrolyte migrated towards the surface of TiO_2 NT arrays under electrical field force and were reduced to Cu^+ ions by the reduction potential. The reaction of Cu^+ ions with H_2O molecules produced Cu_2O particles. The wall of TiO_2 naontubes worked as nucleation centers and the Cu^+ ions gradually aggregated in these nucleation centers and served for the growth of Cu_2O crystals. The growth of Cu_2O crystals was mainly along the normal direction of (100) and (111) planes. At a low deposition current (0.2 mA/cm^2), the growth rate of (111) plane was faster than that of (100) plane slightly and the migration ability of Cu^+ was low and, as a result, the branched, truncated octahedral shapes of Cu_2O particles were obtained. As the deposition current density increased to 0.5 mA/cm^2, the (111) plane became the sole growth plane, which resulted in the formation of integrated octahedron Cu_2O particles. With the deposition current further increasing, the formed octahedron Cu_2O particles overlap each other due to the limited space on the surface of the A-TNT.

XRD analysis shows that anatase TiO_2 formed on Ti plates for the A-TNT samples (Fig.3(a)), and an increasing amount of cuprite formed on the A-TNTs for samples deposited with increasing current densities (Fig.3(b)-(e)). Aside from the diffraction peaks assigned to metallic Ti, anatase TiO_2 and cuprite, one minor peak marked with * is found in D-TNTs and is assigned to (002) and ($\bar{1}$11) planes of CuO (in the CuO crystal, the (002) and ($\bar{1}$11) planes have a same interplanar spacing, and hence the diffraction peaks locate at the same position, PDF No. 45-0937), indicating that a small amount of CuO also formed. According to the paper[21], CuO clusters can also act as an effective co-catalyst in enhancing photocatalytic activity of TiO_2. So the formation of CuO could have a positive effect on the photocatalytic activity of TiO_2. There are no evident shifts in the peak positions of TiO_2 for all samples, suggesting that the deposited Cu_2O particles do not incorporate into the lattice of TiO_2, and are probably attached on the surface of TiO_2 crystalline grains. This result is similar to that of Yu *et al*[22], who reported the $Cu(OH)_2$ cluster modified TiO_2.

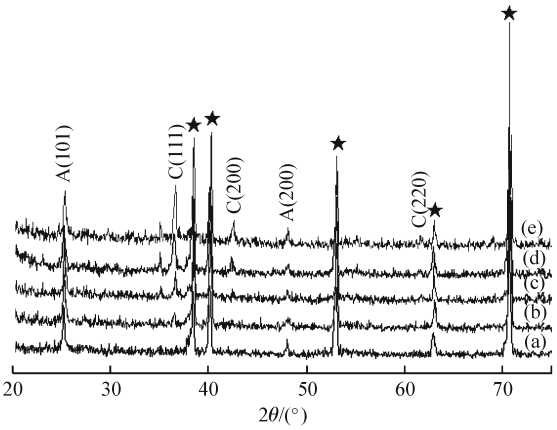

Fig.3 XRD patterns of (a) as-prepared A-TNT arrays and (b) to (e) D-TNT arrays with different deposition current densities: (b) J=0.2 mA/cm^2, (c) J=0.5 mA/cm^2, (d) J=1.0 mA/cm^2 and (e) J=1.5 mA/cm^2 (★ titanium, * copper oxide, "A" and "C" stand for anatase titania and cuprous oxide, respectively)

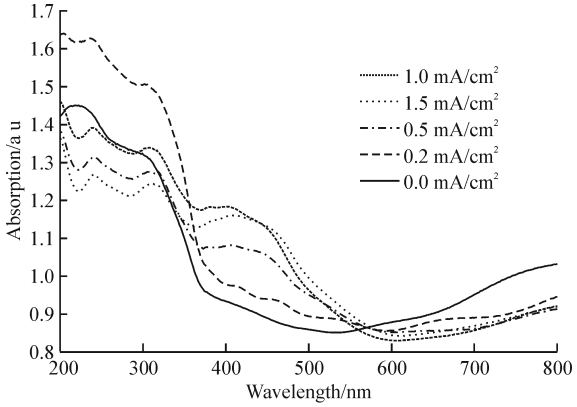

Fig.4 UV-vis/DR spectra of A-TNT arrays and D-TNT arrays

Fig.4 shows the UV–Vis/DR spectra of the A-TNT and D-TNT arrays. All the samples have a significant absorption in the ultraviolet region below 380 nm. There is no obvious change in the absorption edge of the A-TNT and D-TNT arrays, indicating that Cu_2O was not incorporated into the lattice of TiO_2 but was deposited on its surface only. This is due to the charges of Ti^{4+} and Cu^{2+} are not balanced, which is similar to a previous report[21]. In the visible light region from 380 to 580 nm, the A-TNT arrays also show a certain light absorption, which is probably caused by the trapped charge carriers or the absorption of incident light by TiO_2 nanotube arrays[23].

The D-TNT arrays show a stepwise enhancement in light absorption as the deposition current density increases from 0.2 to 1.0 mA/cm^2. When the deposition

current density reaches 1.0 mA/cm^2, the sample shows a maximum absorption value at 410 nm wavelength. It is indicated from the results of SEM observation and XRD patterns that the higher the deposition current is, the more the Cu_2O particles is produced and the stronger the absorption of the D-TNT arrays obtained in the visible-light region. However, when the deposition current density is further increased to 1.5 mA/cm^2, the absorption decreases slightly.

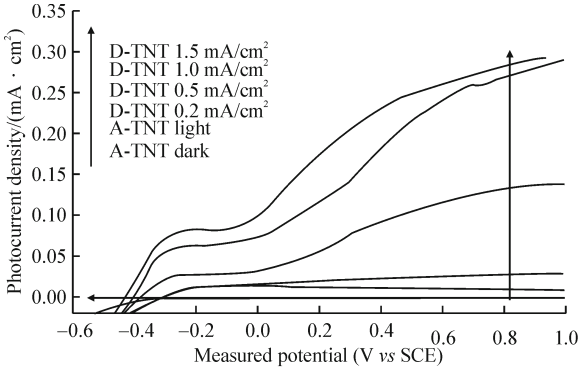

Fig. 5 *I-V* curves of A-TNT and D-TNT arrays

The I-V characteristics of the A-TNT and D-TNT arrays measured in a 0.5 M Na_2SO_4 electrolyte as a function of the deposition current density in the dark and under visible light illumination are shown in Fig.5. In the dark, the current densities of all samples are not any different from each other, nearly to zero at 1.0 V (so here only the dark current curve of the A-TNT is shown). Under visible light irradiation, the A-TNT array exhibits a somewhat higher photocurrent density than that in the dark. However, the D-TNT arrays show notable increases in photocurrent densities and the higher the deposition current density is, the more the photocurrent density increases. That means the photocurrent of the D-TNT arrays increases with increasing Cu_2O content. The photocurrent densities of the samples deposited with current densities of 1.0 and 1.5 mA/cm^2 are more than 30 times as high as that of the A-TNT sample at the applied potentials of 1.0 V. The photocatalytic activity of the D-TNT arrays are dependent mainly on the generation and separation of photo-induced electron and hole pairs and the efficiency of electron-transfer between the semiconductors[23]. The higher photocurrent density means the more photogenerated electron-hole pairs produced and separated. With further increasing of the deposition current density from 1.0 to 1.5 mA/cm^2, the photocurrent did not increase any more. This is because the excess amount of Cu_2O can not produce more photogenerated electron-hole pairs or the induced photogenerated electron-hole pairs could not separate effectively. It is quite interesting that the I-V curve of the D-TNT samples under visible light irradiation shows a distinct plateau in the region between about −0.3 and 0 V when the deposition current density is 0.5 mA/cm^2 or above. The enhanced photocurrent density of the loaded TNT arrays means that visible light induces the generation of more electron/hole pairs which may be easily separated and transported within the heterojunction materials. Fig.5 also shows that the modification of Cu_2O results in a negative shift of the zero-current potential, as indicated by the arrow. This further confirms that the modification of Cu_2O can enhance the separation of photogenerated electron-hole pairs, which is in basic agreement with the results of Kuang *et al*[24], who reported that the modification of Fe_2O_3 on TiO_2 nanotube arrays resulted in a negative shift of the zero-current potential. Furthermore, the short-circuit current also increases significantly as the deposition current increases, as can also be seen in Fig.5.

4 Conclusions

Cu_2O modified TNT can be easily fabricated by synthesizing TiO_2 nanotube arrays in an anodization process followed by galvanostatic pulse electrodeposition of Cu_2O in a cupric acetate aqueous solution. This composite electrode material has the advantages of both easily producing photoinduced electrons by visible light in Cu_2O and the ability to transport these photoinduced electrons in the TiO_2 nanotubes. Experimental results demonstrated that the presence of Cu_2O significantly enhances the visible light response of TiO_2. A distinct plateau is presented on the I-V curve of Cu_2O-modified TNT arrays under visible light irradiation in the region between approximately −0.3 and 0 V. Both the open-circuit voltage and the short-circuit current increase with increasing Cu_2O deposition, and the remarkable improvement in the photocurrent density under visible light irradiation further confirms that the TiO_2/Cu_2O heterojunctions promote the separation and transfer of photoinduced electrons and hence inhibit combination with holes. It has important significance for the TiO_2 application.

References

[1] S Iijima. Helical Microtubules of Graphitic Carbon[J]. *Nature*, 1991, 354(6348): 56-58

[2] S P Albu, A Ghicov, J M Macak, *et al.* Self-organized, Free-standing TiO_2 Nanotube Membrane for Flow-through Photocatalytic Applications[J]. *Nano Lett*., 2007, 7(5): 1 286-1 289

[3] Z Y Liu, X T Zhang, S Nishimoto, *et al*. Efficient Photocatalytic Degradation of Gaseous Acetaldehyde by Highly Ordered TiO_2 Nanotube Arrays[J]. *Environ. Sci. Technol*., 2008, 42(22): 8 547-8 551

[4] L K Tan, M K Kumar, H Gao, *et al.* Transparent, Well-aligned TiO_2 Nanotube Arrays with Controllable Dimensions on Glass Substrates for Photocatalytic Applications[J]. *ACS Appl. Mater. Interfaces*, 2010, 2(2): 498-503

[5] Z H Xu, J G Yu, G Liu. Enhancement of Ethanol Electrooxidation on Plasmonic Au/TiO_2 Nanotube Arrays[J]. *Electrochem. Commun*., 2011, 13(11): 1 260-1 263

[6] J H Park, S Kim, A J Bard. Novel Carbon-doped TiO_2 Nanotube Arrays with High Aspect Ratios for Efficient Solar Water Splitting[J]. *Nano Lett*., 2006, 6(1): 24-28

[7] G K Mor, K Shankar, C A Grimes, *et al.* Use of Highly-ordered TiO_2 Nanotube Arrays in Dye-sensitized Solar Cells[J]. *Nano Lett*., 2006, 6(2): 215-218

[8] C C Tsai, H Teng. Regulation of the Physical Characteristics of Titania Nanotube Aggregates Synthesized from Hydrothermal Treatment[J]. *Chem. Mater*., 2004, 16(22): 4 352-4 358

[9] D A Wang, F Zhou, Y Liu, *et al.* Synthesis and Characterization of Anatase TiO_2 Nanotubes with Uniform Diameter from Titanium Powder[J]. *Mater. Lett.*, 2008, 62(12-13): 1 819-1 822

[10] R A Caruso, J H Schattka, A Greiner. Titanium Dioxide Tubes from Sol-gel Coating of Electrospun Polymer Fibers[J]. *Adv. Mater*., 2001, 13(20): 1 577-1 579

[11] J H Jung, H Kobayashi, S Shinkai, *et al.* Creation of Novel Helical Ribbon and Double-layered Nanotube TiO_2 Structures Using an Organogel Template[J]. *Chem. Mater*., 2002, 14(4): 1 445-1 447

[12] D W Gong, C A Grimes, O K Varghese, *et al.* Titanium Oxide Nanotube Arrays Prepared by Anodic Oxidation[J]. *J. Mater. Res*., 2001, 16(12): 3 331-3 334

[13] G K Mor, O K Varghese, M Paulose, *et al.* Fabrication of Tapered, Conical-shaped Titania Nanotubes[J]. *J. Mater. Res*., 2003, 18(11): 2 588-2 593

[14] X Quan, S G Yang, X L Ruan, *et al.* Preparation of Titania Nanotubes and Their Environmental Applications as Electrode[J]. *Environ. Sci. Technol*., 2005, 39(10): 3 770-3 775

[15] A E Rakhshani. Preparation, Characteristics and Photovoltaic Properties of Cuprous Oxide—a Review[J]. *Solid State Electron.*, 1986, 29(1): 7-17

[16] P E de Jongh, D Vanmaekelbergh, J J Kelly. Photoelectrochemistry of Electrodeposited Cu_2O[J]. *Electrochemi. Soc*., 2000, 147(2): 486-489

[17] T Mahalingam, G Ravi, J P Chu, *et al*. Characterization of Pulse Plated Cu_2O Thin Films[J]. *Surf. Coat. Tech*., 2003, 168(2-3): 111-114

[18] Y Hou, X Y Li, G H Chen, *et al.* Photoelectrocatalytic Activity of a Cu_2O-loaded Self-organized Highly Oriented TiO_2 Nanotube Array Electrode for 4-Chlorophenol Degradation[J]. *Environ. Sci. Technol*., 2009, 43(3): 858-863

[19] G K Mor, O K Varghese, C A Grimes, *et al.* Transparent Highly Ordered TiO_2 Nanotube Arrays via Anodization of Titanium Thin Films[J]. *Adv. Funct. Mater.*, 2005, 15(8): 1 291-1 296

[20] L Huang, S Zhang, F Peng, *et al.* Electrodeposition Preparation of Octahedral-Cu_2O-loaded TiO_2 Nanotube Arrays for Visible Light-driven Photocatalysis[J]. *Scripta Mater*., 2010, 63(2): 159-161

[21] J G Yu, Y Hai, M Jaroniec. Photocatalytic Hydrogen Production over CuO-modified Titania[J]. *J. Colloid Interface Sci.*, 2011, 357(1): 223-228

[22] J G Yu, J R Ran. Facile Preparation and Enhanced Photocatalytic H_2-production Activity of $Cu(OH)_2$ Cluster Modified TiO_2[J]. *Energy Environ. Sci*., 2011, 4(4), 1 364-1 371

[23] Z H Xu, J G Yu. Visible-light-induced Photoelectrochemical Behaviors of Fe-modified TiO_2 Nanotube Arrays[J]. *Nanoscale*, 2011, 3(8): 3 138-3 144

[24] S Y Kuang, S L Luo, Q Y Cai, *et al.* Fabrication, Characterization and Photoelectrochemical Properties of Fe_2O_3 Modified TiO_2 Nanotube Arrays[J]. *Appl. Surf. Sci*., 2009, 255(16): 7 385-7 388